Resendiz Lira, P. A., Marchand, R., Burchill, J., Förster, M. (2019): Determination of Swarm Front Plate's Effective Cross Section From Kinetic Simulations. - *IEEE Transactions on Plasma Science*, *47*, 8, pp. 3667—3672.

DOI: http://doi.org/10.1109/TPS.2019.2915216

Determination of Swarm front plate's effective cross section from kinetic simulations

Pedro Alberto Resendiz Lira, Richard Marchand, Johnathan Burchill, Matthias Förster

***Abstract*—The front plates and embedded particle sensor shells that are part of the Electric Field Instrument (EFI) on the Swarm satellites have recently been used as planar Langmuir probes, as an additional diagnostic tool to infer environment parameters. The interpretation of measured currents in terms of the plasma density or incoming flow speed, however, requires a knowledge of the front plate effective cross section A_{eff}. Measurements made under various space plasma conditions have led to the conclusion that this cross section is generally larger than the known geometrical cross section A_{geo}. Interpretations of measurements have thus been made using fixed relative enhancements of A_{geo} ranging from 8 to 17%. In this paper results from kinetic simulations are presented, from which the effective cross section can be determined over a range of plasma parameters. These are used to shed light on the physical mechanisms responsible for this enhancement, and construct an empirical fit to the relative enhancement δ, where $A_{eff} = A_{geo}(1 + \delta)$, and in turn enable improvements in the accuracy of inferred plasma parameters.**

***Index Terms*—Space Plasma, Swarm satellites, kinetic simulations, planar Langmuir probe**

I. Introduction

LANGMUIR probes have been used extensively to diagnose plasma in laboratory and space. The interpretation of probe measurements is based generally on relatively simple analytic models that cannot account for the many factors affecting measurements. As a result the inference of plasma parameters such as the density and temperature comes with appreciable uncertainties. Indeed many theoretical studies have been made over the years [1], [2], [3], [4], [5], [6], but none is capable to account for all the physical effects affecting probe measurements under realistic conditions. Recently numerical simulations have been used to compute probe characteristics under increasingly more realistic conditions,[7], [8], [9]. While such simulations can provide useful insight, the computational effort that they require renders them inapplicable for real time interpretation of probe measurements. As a result, probe measurements are generally interpreted using relatively simple analytic expressions, resulting in uncertainties ranging from a few percent, to more than 100 % [10], [11]. The case of interest here is that of the front plate on Swarm when it is used as planar Langmuir probes. Each of the three Swarm spacecraft is equipped with a front plate in which two Thermal Ion Imagers (TII) are embedded as part of the Electric Field Instrument (EFI) [12]. When the ion imagers are not in operation, the current collected by the front plate and the shells of the TII can be measured at a sample rate of 16 Hz, and the front plate can be used as fixed-bias Langmuir probe. With e being the unit charge and considering that plasma flow is supersonic in the spacecraft reference frame, the relation for the ion current collected when the probe is operated in the ion saturation region (typically $V_{bias} = -3.5$ V with respect to the spacecraft)

$$I = env_{\perp}A_{geo} \tag{1}$$

provides an approximate relation between the measured current I, the plasma density n and the incoming plasma flow speed $v_{\perp}$ in the direction perpendicular to the plate, given the known geometrical cross section of the plate A_{geo}. Measurements interpreted on the basis on eq. 1 however, suggest that the geometrical cross section A_{geo} has to be increased by several percent in order to reconcile the results with those of other independent measurements [13]. Indeed increases in the effective front plate cross section by 8 up to 17 % were suggested to reduce the discrepancies with other measurements. While a step in the right direction, these ad hoc fixed increases suggest that a closer look should be given to explain them in terms of underlying physical processes. The goal of this work is therefore to carry out simulations to quantitatively determine the relative enhancement

$$\delta = \frac{A_{eff} - A_{geo}}{A_{geo}} = \frac{I}{env_{\perp}A_{geo}} - 1 \tag{2}$$

over a range of relevant ionospheric plasma parameters, and from there, better understand the physical processes at play, and construct an empirical model to approximate δ under different space environment conditions.

The remainder of the paper briefly describes the computational approach used to carry out the simulations, followed by a presentation of our results and the construction of an empirical model for calculating the relative enhancement δ. Finally, Section IV contains a summary of our findings and some concluding remarks.

II. Methodology

The current collected by a Swarm front plate is calculated for several ionospheric environment conditions, by carrying out kinetic simulations with PTetra [14], [15]. In the simulations a reduced Swarm geometry shown in Fig. 1 is considered, which accounts for a segment of the main spacecraft body, the front plate, the shells covering the thermal ion imagers, and the two spherical Langmuir probes. While greatly simplified, the

P. Resendiz Lira and R. Marchand are with the Department of Physics, University of Alberta, Alberta Canada.

J. Burchill is with the Department of Physics and Astronomy, University of Calgary, Alberta Canada.

M. Förster is with the GFZ German Research Centre for Geosciences in Potsdam, Germany, and the Max Planck Institute for Solar System Research in Gottingen, Germany.

Manuscript received October 1, 2018; revised a later date

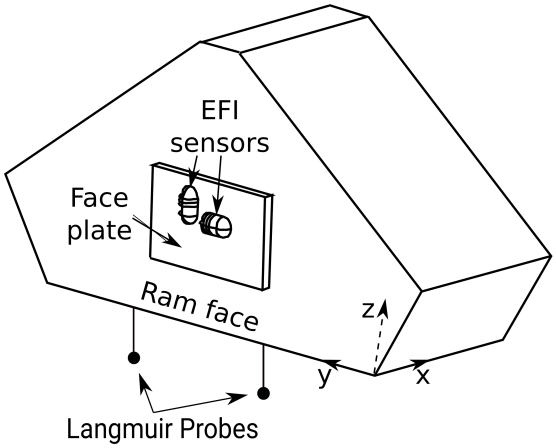

Fig. 1. Illustration of a simplified Swarm geometry with front plate and TII shells. In the simulations the front plate is a rectangle with an area of $351 \times 229\ mm^2$.The thickness of the plate is 3.175 mm while the separation between the plate and the satellite bus is 21.825 mm. The Langmuir probe radius is 4 mm. The schematic of the spherical probes in the figure are not to scale.

assumption is that this geometry is sufficient to study the interaction between the front plate and incoming supersonic plasma when the front plate is biased sufficiently negatively with respect to the spacecraft bus. In the simulations, both electron and ion species are treated fully kinetically using the Particle-In-Cell (PIC) approach, and the electric sheath surrounding the front plate and bus are calculated self-consistently. Simulations are made using approximately 163 to 549 million particles in an unstructured adaptive tetrahedral mesh with numbers of elements (tetrahedra) ranging from approximately 2.1 to 4.6 million. The simulation domain is a cylinder of approximately 7 m long, with a radius of approximately 1 m. Several cases are considered in which the temperature, the density, the ion composition, and the satellite floating potential are varied. In this study, a fixed plasma flow velocity of 7673 m/s from the ram direction is considered. For simplicity, photoelectron emission and secondary electron emission are not accounted for. This simplification should be valid when the spacecraft is on the night side of their orbit, or in higher density regions of the ionosphere, where collected ion currents exceed those from photoelectron emission. Simulations have been made with and without the inclusion of representative geomagnetic field, and it was found that for the supersonic flows ($v \sim 7673$ m/s) considered and the relatively large ion gyroradii (~ 1 m for H^+ ions and ~ 4 m for O^+) the inclusion of magnetic fields had no significant effect. Similarly, simulations have been made by adding transverse (in directions parallel to the plate) flow velocities up to 1000 m/s, in which the relative enhancement remains the same within two significant figures. For that reason, only simulations with a flow velocity in the direction perpendicular to the plate are considered. Different ion compositions have also been considered including pure O^+ plasma and O^+ with representative fractions of lighter minority ions as obtained from the International Reference Ionosphere (IRI) model [16]. The strength and thickness of the electric sheath surrounding the front plate has an important

n	Te	m_{eff}	λ_D	V	I	δ_{sim}	ϵ
$10^{10}m^{-3}$	eV		mm	V	μA	%	%
3.16	0.070	7.35	11.06	-3.70	3.504	12.24	0.0
3.16	0.070	7.35	11.06	-4.50	3.537	13.28	0.4
3.16	0.070	7.35	11.06	-5.50	3.575	14.49	1.1
10.00	0.070	5.85	6.22	-3.70	10.732	8.61	0.3
10.00	0.070	5.85	6.22	-4.50	10.824	9.54	0.6
10.00	0.070	5.85	6.22	-5.50	10.903	10.34	0.4
31.6	0.070	4.10	3.50	-3.70	33.433	7.07	1.0
31.6	0.070	4.10	3.50	-4.50	33.629	7.70	1.4
31.6	0.070	4.10	3.50	-5.50	33.879	8.50	**1.7**
63.2	0.082	13.71	2.68	-3.73	64.227	**2.84**	1.6
63.2	0.082	13.71	2.68	-4.50	64.549	3.36	1.0
63.2	0.082	13.71	2.68	-5.50	64.936	3.98	0.4
1.00	0.156	8.29	29.36	-4.01	1.182	19.58	0.9
1.00	0.156	8.29	29.36	-4.50	1.187	20.15	0.1
1.00	0.156	8.29	29.36	-5.50	1.198	**21.25**	**1.7**
3.16	0.140	11.40	15.65	-3.95	3.451	10.53	0.3
3.16	0.140	11.40	15.65	-4.50	3.477	11.35	0.1
3.16	0.140	11.40	15.65	-5.50	3.519	12.70	0.2
10.0	0.140	12.99	8.80	-3.94	10.488	6.14	0.9
10.0	0.140	12.99	8.80	-4.50	10.551	6.78	0.5
10.0	0.140	12.99	8.80	-5.50	10.656	7.84	0.0
31.6	0.140	15.88	4.95	-3.94	32.355	3.61	1.3
31.6	0.140	15.88	4.95	-4.50	32.490	4.05	0.9
31.6	0.140	15.88	4.95	-5.50	32.710	4.75	0.3
3.16	0.210	12.57	19.16	-4.22	3.461	10.83	0.1
3.16	0.210	12.57	19.16	-4.50	3.473	11.23	0.2
3.16	0.210	12.57	19.16	-5.50	3.513	12.52	0.3
10.0	0.220	11.28	11.03	-4.25	10.579	7.06	0.1
10.0	0.220	11.28	11.03	-4.50	10.604	7.31	0.2
10.0	0.220	11.28	11.03	-5.50	10.699	8.27	0.5
10.0	0.280	15.96	12.44	-4.49	10.535	6.61	0.2
10.0	0.280	15.96	12.44	-5.50	10.635	7.63	0.4

TABLE I

SUMMARY OF SIMULATION PARAMETERS WITH COMPUTED FRONT PLATE COLLECTED CURRENTS, RELATIVE ENHANCEMENT δ AND ABSOLUTE ERRORS $\epsilon = |\delta_{sim} - \delta_{model}|$ IN PREDICTED ENHANCEMENTS OBTAINED WITH MODEL EQUATION 4. THE SMALLEST AND LARGEST VALUES OF δ_{sim}, AND THE LARGEST RELATIVE ERRORS ϵ ARE IN BOLD.

role in ion collection. The sheath around the front plate depends on the potential of the plate with respect to the background plasma, $V = V_{bias} + V_{float}$. Since the front plate is typically operated at a fixed bias voltage of -3.5 V (V_{bias}) with respect to the spacecraft, different floating potentials were assumed in order to account for different possible plate potentials with respect to surrounding plasma (-2 V, -1 V, and one calculated self-consistenly from simulations). Typical values for the spacecraft floating potential estimated from in situ measurements are around -2 V in the simulations. In each case the effective cross section

$$A_{eff} = \frac{I}{env_{\perp}} \tag{3}$$

has been calculated, and the relative enhancement δ has been determined from eq. 2. Table I summarizes the cases considered, with the corresponding relative enhancements δ. The table shows, consistently with suggestions from observations, that the effective plate cross section is indeed larger than the geometrical cross section, corresponding to positive values of δ. We also note that the values of the relative enhancements are in the range 2.84 to 21.25 %, consistent with the empirical values of 8 to 17 % mentioned above, and used when processing front plate collected currents. The next step consists of constructing an empirical analytic expression that can approximate the tabulated values of δ in the range of parameters considered.

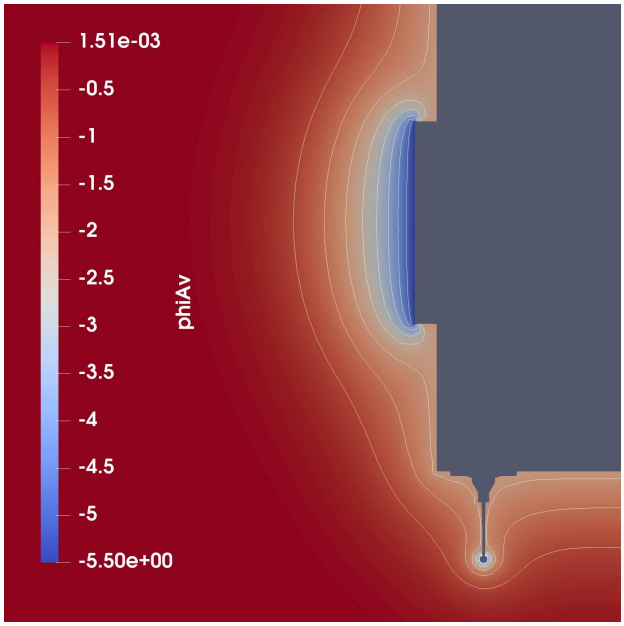

Fig. 2. Curved equipotentials in around the front plate and Langmuir probe.

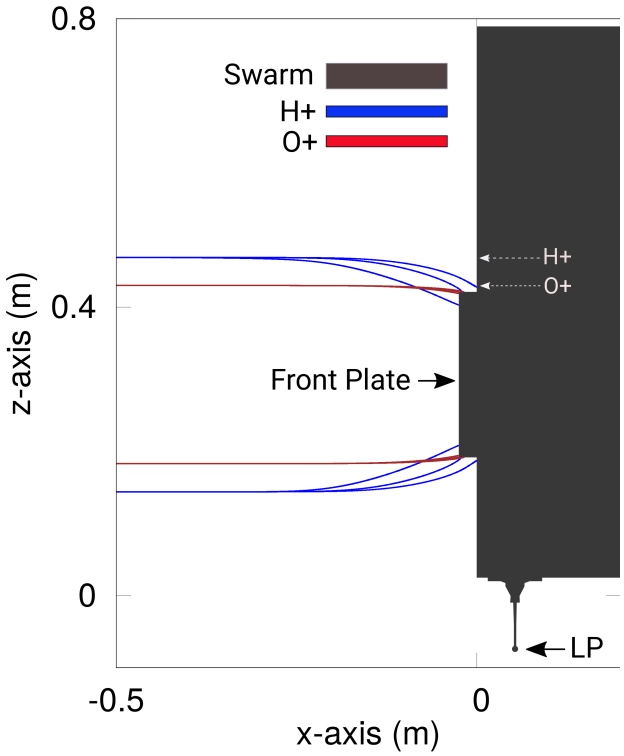

Fig. 3. Ion trajectories deflected near the front plate, due to curved equipotentials around the perimeter. Both species are aimed slightly below or above (dashed arrows) the plate with velocities exactly from the ram direction. Three speeds are considered corresponding to v_{ram}, and $v_{ram} \pm v_{th}$ with $v_{th} = (2kT/m)^{1/2}$ being the species thermal speed. Particles with the lower speed $(v_{ram} - v_{th})$ are deflected the most, and the ones with the higher speed $(v_{ram} + v_{th})$ are deflected the least.

Referring to Figs. 3 and 4, the enhancement in the collected ion currents is seen to be caused by electric fringe effects at the plate perimeter, whereby electric fields associated with curved equipotential surfaces near the edge shown in Fig. 2, deflect incident ions towards the plate. The electric potential profile shown in Fig. 2 corresponds to the case in Table I for which enhancement is the largest, at 21.25 %, and plasma density is the lowest at $n = 1 \times 10^{10} m^{-3}$. The floating potential was set to $-2\ V$, whereas the plate is biased to $-3.5\ V$ with respect to the spacecraft, thus, the plate is biased to $-5.5\ V$ with respect to background plasma. The particle trajectories in Fig. 3 and 4 were calculated using the electric field obtained from the equipotential surfaces shown in Fig. 2. In Fig. 3, twelve plasma particles, six Hydrogen ions and six Oxygen ions, were lanched from the boundary towards the plate with velocities of magnitude equal to the ram velocity plus or minus their respective thermal speed. In all cases, particles would miss the plate in the absence of the sheath electric field. The presence of the electric field directed toward the plate, however, deflects a fraction of these incoming particles to the edge of the plate where they add to the collected current and thus contribute to the relative enhancement of the front plate effective cross section. Similarly in Fig. 4, thirty eight particles (nineteen H^+ and nineteen O^+) injected at the upstream boundary, from different angles with speeds equal to the ram speed plus their respective species thermal speed. All particles are aimed a few centimeters above the front-plate and would miss the plate in the absence of the sheath electric field but, as seen in the figure, (in the presence of the field,) many are deflected to the plate where they add to the collected ion current.

It was found that the relative enhancements δ in Table I can be approximated with good accuracy analytically. Several expressions with adjustable parameters have been tried, and the one that was found to best reproduce our computed enhancement is given by:

$$I = env_{\perp}A_{geo}\left[1 + \frac{\alpha P \lambda_D}{A_{geo}}\left(1 - \frac{eV}{\frac{1}{2}m_{eff}v_{\perp}^2} - \beta\frac{eV}{kT_e} - \frac{\gamma}{eV}\frac{e^2}{4\pi\epsilon_0\lambda_D}\right)\right], \quad (4)$$

where P is the perimeter of the plate (the sum of the length of all sides), V is the plate potential with respect to background plasma, T_e is the electron temperature, and the electron Debye length λ_D is given by $(\epsilon_0 kT_e/e^2 n)^{1/2}$. α, β, and γ are fitting parameters. The effective thickness of the deflecting region around the plate is taken to be proportional to the scaled electron Debye length λ_D. In eq. 4, the term $(eV)/(\frac{1}{2}m_{eff}v_{\perp}^2)$ is consistent with the fact that less energetic ions are deflected more by sheath electric fields, and that for a given incident particle energy, larger attractive voltages lead to stronger particle deflections. The term multiplying β accounts for the increase in the sheath thickness surrounding the plate, as the ratio eV/kT increases, while the one multiplying γ was found purely empirically to improve the accuracy of the fit. In eq. 4,

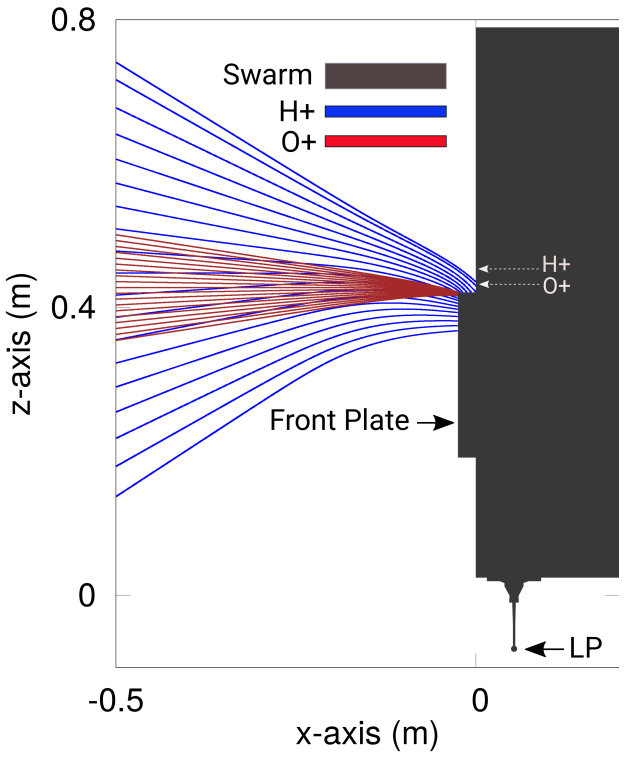

Fig. 4. O^+ and H^+ ion trajectories deflected near the front plate due to curved equipotentials around the perimeter. In all cases, the magnitude of the incident velocity is equal to $\sqrt{(v_{ram}^2 + v_{th}^2)}$, where $v_{th} = (2kT/m)^{1/2}$ is the ion thermal speed. The incoming particles have different incident angle. The arrows show where H^+ and O^+ ions would impact if they were undeflected.

the effective mass is defined by

$$\frac{1}{m_{eff}} = \sum_{i=1}^{N} \frac{n_i}{n_{tot}} \frac{1}{m_i} \tag{5}$$

where, for a multiple-ion species plasma, n_i is the density of species i and n_{tot} is the total ion density. From eq. 4 and the definition of δ in eq. 2, it follows that the relative enhancement in this model is

$$\begin{aligned} \delta_{model} &= \frac{\alpha P \lambda_D}{A_{geo}} \left(1 - \frac{eV}{\frac{1}{2} m_{eff} v_\perp^2} \right. \\ &- \left. \beta \frac{eV}{kT_e} - \frac{\gamma}{eV} \frac{e^2}{4\pi\epsilon_0 \lambda_D} \right). \end{aligned} \tag{6}$$

The three fitting parameters α, β, and γ in eq. 6 are adjusted so as to minimize the maximum absolute error $|\delta_{sim} - \delta_{model}|$. The optimal values are found to be $\alpha = 0.06929$, $\beta = 0.11552$, and $\gamma = 66.0913 \times 10^6$ for which the maximum absolute error is 1.7 %. The correlation between simulated and model predicted relative enhancements is shown in Fig. 5, and the error in the predictions, defined by $|\delta_{sim} - \delta_{model}|$ are listed in Table I for reference. The scatter in this plot may seem disappointing, but as shown below, all other relevant

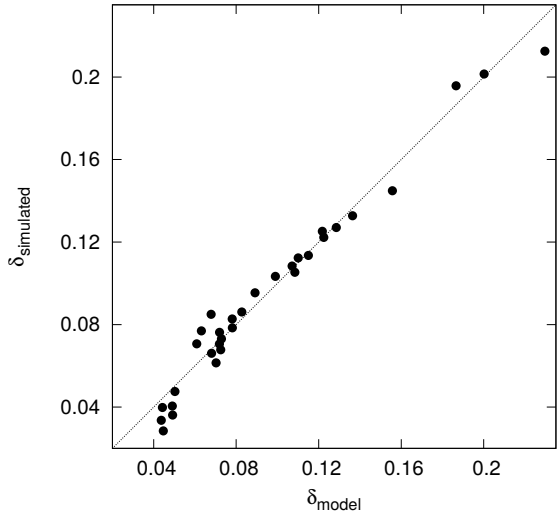

Fig. 5. Correlation between model predicted relative enhancement δ_{model} and values computed from simulations δ_{sim}. For reference the dashed line shows a perfect one-to-one correlation.

parameters being known, the model does allow an estimate of the density within approximately 2 %. This indeed follows, from eq. 3 from which

$$\begin{aligned} n &= \frac{I}{A_{eff} e v_\perp} = \frac{I}{A_{geo}(1+\delta_{sim}) e v_\perp} \\ &= \frac{I}{A_{geo}(1+\delta_{model} \pm \epsilon) e v_\perp}, \end{aligned} \tag{7}$$

where ϵ is the error in the model prediction. The variation in n associated with an uncertainty of $\pm\epsilon$ is then

$$\begin{aligned} \Delta n &= \frac{1}{2} \frac{I}{A_{geo} e v_\perp} \left(\frac{1}{1+\delta_{model} - \epsilon} - \frac{1}{1+\delta_{model} + \epsilon} \right) \\ &= \frac{I}{A_{geo} e v_\perp} \frac{\epsilon}{(1+\delta)^2 - \epsilon^2} = \frac{n(1+\delta)}{(1+\delta)^2 - \epsilon^2} \times \epsilon, \end{aligned} \tag{8}$$

from which

$$\frac{\Delta n}{n} = \frac{(1+\delta)}{(1+\delta)^2 - \epsilon^2} \times \epsilon. \tag{9}$$

Given the relative enhancements and errors listed in Table I, the fraction multiplying ϵ can be seen to be lower than unity in all cases. It then follows that the relative error in the inferred density is at most ϵ. Taking the largest error in the table we conclude that, all other parameters being known, eq. 4 can be used to predict the plasma density with 2 % accuracy over the simulation conditions considered.

III. Discussion

It was shown in Sec. II that, within the range of parameters considered, the empirical formula eq. 4 can be used to determine the plasma density within $\sim$ 1.7 % accuracy, given accurate numerical values of other parameters. This can

be done explicitly by solving for n in terms of the other parameters in eq. 4. After some algebra it follows that

$$n = \left\{ \left[-\frac{\alpha P}{A_{geo}} \sqrt{\frac{\epsilon_0 k T_e}{e^2}} \left(1 - \frac{eV}{\frac{1}{2} m_{eff} v_\perp^2} - \beta \frac{eV}{kT_e} \right) + \left[\left(\frac{\alpha P}{A_{geo}} \right)^2 \frac{\epsilon_0 k T_e}{e^2} \left(1 - \frac{eV}{\frac{1}{2} m_{eff} v_\perp^2} - \beta \frac{eV}{kT_e} \right)^2 - 4 \left(1 - \frac{\alpha P}{A_{geo}} \frac{\gamma}{eV} \frac{e^2}{4\pi\epsilon_0} \right) \left(\frac{I}{e v_\perp A_{geo}} \right) \right]^{\frac{1}{2}} \right] \times \frac{1}{2} \left(1 - \frac{\alpha P}{A_{geo}} \frac{\gamma}{eV} \frac{e^2}{4\pi\epsilon_0} \right)^{-1} \right\}^2 . \quad (10)$$

where the fitting parameters α, β, and γ are determined in the previous section. The point to note here is that a model based on eq. 10, or equivalently on eq. 7, depends explicitly on four unknown plasma parameters. These are the electron temperature T_e, the plasma speed $v_\perp$ in the ram direction, the effective ion mass m_{eff} and the spacecraft floating potential V_{fl}. The dependence on V_{fl} follows from the fact that the plate potential V with respect to background plasma is the sum of the floating potential and the known bias potential V_{bias} : $V = V_{fl} + V_{bias}$. Therefore while it is possible in principle to use eq. 7 to infer the density accurately in the parameter space considered, the skill of the model would depend on the accuracy with which other parameters can be determined. It is not the intent in this paper to discuss other measurements made on Swarm, but suffice it to mention that the electron temperature, the density, and satellite floating potential, can in principle be obtained from the two spherical Langmuir probes [17], [12]. However the effective mass (or relative ion densities) and the plasma flow velocity from the ram direction are not measured independently. It therefore follows that the interpretation of measurements of the collected ion current by the front plate, might involve more unknown plasma parameters than there are independent measurements.

In closing it is interesting to compare values obtained from our model eq. 6 with values inferred using fixed relative enhancements $\delta = 17$ %, 12 % or 8 %. In Table II comparisons are made between relative errors in densities based on these three fixed values, and from our model. While the relative error resulting from a fixed δ can be smaller in some cases, the maximum relative error (in bold) is appreciably less when our model is used, which implies that, in the range of parameters considered, more accurate inference of the density can be made by using eq. 7 or equivalently eq. 10. The results shown in the previous section confirm that an enhancement in the collection area of the front plate as planar Langmuir probe exists. Our proposed model for the enhancement depends on the geometry of the plate, the percentage of light ions in the plasma and their kinetic energy, as well as the electric sheath surrounding the front plate.

n	T	m_{eff}	λ_D	$\delta_{17\%}$	$\delta_{12\%}$	$\delta_{8\%}$	δ_{model}
$10^{10} m^{-3}$	eV		mm	%	%	%	%
3.16	0.070	7.35	11.06	-4.2	+0.2	+3.8	+0.7
3.16	0.070	7.35	11.06	-3.3	+1.1	+4.7	+0.7
3.16	0.070	7.35	11.06	-2.2	+2.2	+5.7	+0.5
10.00	0.070	5.85	6.22	-7.7	-3.1	+0.6	+0.5
10.00	0.070	5.85	6.22	-6.8	-2.2	+1.4	+0.9
10.00	0.070	5.85	6.22	-6.0	-1.5	+2.2	+1.0
31.6	0.070	4.10	3.50	-9.3	-4.6	-0.9	+0.7
31.6	0.070	4.10	3.50	-8.6	-4.0	-0.3	+1.2
31.6	0.070	4.10	3.50	-7.8	-3.2	+0.5	+1.6
63.2	0.082	13.71	2.68	**-13.7**	**-8.9**	-5.0	**-1.7**
63.2	0.082	13.71	2.68	-13.2	-8.4	-4.5	-0.9
63.2	0.082	13.71	2.68	-12.5	-7.7	-3.9	-0.3
1.00	0.156	8.29	29.36	+2.2	+6.3	+9.7	+1.3
1.00	0.156	8.29	29.36	+2.6	+6.8	+10.1	+0.5
1.00	0.156	8.29	29.36	+3.5	+7.6	**+10.9**	-0.9
3.16	0.140	11.40	15.65	-5.9	-1.3	+2.3	+0.1
3.16	0.140	11.40	15.65	-5.1	-0.6	+3.0	+0.4
3.16	0.140	11.40	15.65	-3.8	+0.6	+4.2	+0.6
10.0	0.140	12.99	8.80	-10.2	-5.5	-1.8	-0.8
10.0	0.140	12.99	8.80	-9.6	-4.9	-1.1	-0.3
10.0	0.140	12.99	8.80	-8.5	-3.9	-1.5	+0.4
31.6	0.140	15.88	4.95	-12.9	-8.1	-4.2	-1.4
31.6	0.140	15.88	4.95	-12.4	-7.6	-3.8	-0.8
31.6	0.140	15.88	4.95	-11.7	-6.9	-3.1	-0.1
3.16	0.210	12.57	19.16	-5.6	-1.1	+2.6	+0.2
3.16	0.210	12.57	19.16	-5.2	-0.7	+2.9	+0.4
3.16	0.210	12.57	19.16	-4.0	+0.5	+4.1	+0.6
10.0	0.220	11.28	11.03	-9.3	-4.6	-0.9	-0.3
10.0	0.220	11.28	11.03	-9.0	-4.4	-0.6	-0.2
10.0	0.220	11.28	11.03	-8.1	-3.4	+0.3	+0.4
10.0	0.280	15.96	12.44	-9.7	-5.1	-1.3	-0.3
10.0	0.280	15.96	12.44	-8.7	-4.1	-0.3	+0.4

TABLE II

LIST OF RELATIVE ERRORS IN THE DENSITIES INFERRED WITH A FIXED RELATIVE ENHANCEMENT δ OF 0.17, $\delta_{17\%}$, 0.12, $\delta_{12\%}$, AND 0.08, $\delta_{8\%}$. THE RIGHTMOST COLUMN GIVES THE RELATIVE ERRORS δ_{model} RESULTING FROM USING OUR MODEL. ALL RELATIVE ERRORS ARE IN PERCENT. POSITIVE AND NEGATIVE VALUES OF δ CORRESPOND RESPECTIVELY TO MODEL OVER-, AND UNDERESTIMATES.

IV. SUMMARY AND CONCLUSIONS

An empirical expression for the current collected by the Swarm front-plate is proposed which reproduces the enhancement of the Swarm EFI front plate as a function of plasma environment parameters. This expression in turn is meant to improve the interpretation of ion current collected by the plate when it is operated as a planar Langmuir probe. The analytic expression for the relative enhancement δ is constructed to best represent the simulation results, and account for the deflection of incoming ions to the plate by fringe electric fields around the plate perimeter. The three fitting parameters in the model were adjusted by minimizing the maximum absolute error in computed relative enhancements δ_{sim} over a range of parameters of relevance to mid latitude ionospheric plasma. Given accurate values for the other parameters, our model can be used to infer the density from measured collected currents, with an accuracy of approximately 2 % in the range of parameters considered. The skill of the model was also compared with predictions making use of fixed (independent of plasma parameters) values of δ. In all cases the maximum relative error computed for the thirty two cases considered, was significantly lower when using δ predicted with our model. It was noted however that, while our model can infer the density from measurements with good accuracy, it does rely on other environment parameters being known with sufficiently good accuracy. Those parameters include the electron temperature, the flow velocity in the ram direction, the effective ion mass, and the spacecraft floating potential. Finally we recognize that

this study is a first step at understanding and quantifying the physical causes of the observed enhancement in the Swarm front plate effective cross section. Our longer term goal being to improve the interpretation of measured currents collected by the front plate, in order to better infer the density and possibly other plasma parameters, we plan to pursue our analysis with the inclusion of more physical processes, and possibly cover a broader range of space environment conditions. Such processes would include photoelectron emission from the satellite, and possibly the front plate when the satellite is exposed to solar radiation, as well as the inclusion of variations in the along track plasma flow velocity. Photoelectron emission from the plate would likely increase the effective positive current collected, and thereby contribute to further enhancing the effective cross section. This enhancement in turn would depend on the orientation of the satellite with respect to the sun and, given electron's relatively small gyro-radii, on the strength and direction of the magnetic field. Variations in the along-track plasma flow velocity would modify the kinetic energy of incoming ions. More energetic ions would be deflected less by the fringe electric fields at the plate, while less energetic ions would be deflected more. This would result in lower and higher relative enhancements respectively. The construction of such a detailed model is beyond the scope of this first exploratory study, and it is intended for future studies.

ACKNOWLEDGMENT

This work was supported in part by the Natural Sciences Engineering Council of Canada, by the Consejo Nacional de Ciencia y Tecnologia, by the Canadian Space Agency, and by the European Space Agency. The simulation results presented here were made possible by computing resources provided by Compute Canada.

REFERENCES

[1] H. M. Mott-Smith and I. Langmuir, "The theory of collectors in gaseous discharges," *Phys. Rev.*, vol. 28, pp. 727–763, Oct 1926. [Online]. Available: https://link.aps.org/doi/10.1103/PhysRev.28.727

[2] J. G. Laframboise, "Theory of spherical and cylindrical Langmuir probes in a collisionless, Maxwellian plasma at rest," Ph.D. dissertation, University of Toronto, 1966.

[3] J.-S. Chang and J. Laframboise, "Probe theory for arbitrary shape in a large debye length, stationary plasma," *The Physics of Fluids*, vol. 19, no. 1, pp. 25–31, 1976.

[4] J. Laframboise and J. Rubinstein, "Theory of a cylindrical probe in a collisionless magnetoplasma," *The Physics of Fluids*, vol. 19, no. 12, pp. 1900–1908, 1976.

[5] J. Rubinstein and J. Laframboise, "Theory of a spherical probe in a collisionless magnetoplasma," *The Physics of Fluids*, vol. 25, no. 7, pp. 1174–1182, 1982.

[6] J. Laframboise and L. Sonmor, "Current collection by probes and electrodes in space magnetoplasmas: A review," *Journal of Geophysical Research: Space Physics*, vol. 98, no. A1, pp. 337–357, 1993.

[7] F. F. Chen, "Numerical computations for ion probe characteristics in a collisionless plasma," *Journal of Nuclear Energy. Part C, Plasma Physics, Accelerators, Thermonuclear Research*, vol. 7, no. 1, p. 47, 1965.

[8] J. Allen, "Probe theory-the orbital motion approach," *Physica Scripta*, vol. 45, no. 5, p. 497, 1992.

[9] A. Bergmann, "Two-dimensional particle simulation of Langmuir probe sheaths with oblique magnetic field," *Physics of Plasmas*, vol. 1, no. 11, pp. 3598–3606, 1994.

[10] I. D. Sudit and R. C. Woods, "A study of the accuracy of various Langmuir probe theories," *Journal of applied physics*, vol. 76, no. 8, pp. 4488–4498, 1994.

[11] A. Hoskinson and N. Hershkowitz, "Effect of finite length on the current–voltage characteristic of a cylindrical Langmuir probe in a multidipole plasma chamber," *Plasma Sources Science and Technology*, vol. 15, no. 1, p. 85, 2006.

[12] D. Knudsen, J. Burchill, S. Buchert, A. Eriksson, R. Gill, J.-E. Wahlund, L. Åhlen, M. Smith, and B. Moffat, "Thermal ion imagers and Langmuir probes in the swarm electric field instruments," *Journal of Geophysical Research: Space Physics*, vol. 122, no. 2, pp. 2655–2673, 2017.

[13] M. Förster, personal communication, 2018.

[14] R. Marchand, "Ptetra, a tool to simulate low orbit satellite-plasma interaction," *IEEE Trans. Plasma Sci. (USA)*, vol. 40, no. 2, pp. 217 – 29, 2012.

[15] R. Marchand and P. A. R. Lira, "Kinetic simulation of spacecraft-environment interaction," *IEEE Transactions on Plasma Science*, 2017.

[16] D. Bilitza, D. Altadill, Y. Zhang, C. Mertens, V. Truhlik, P. Richards, L.-A. McKinnell, and B. Reinisch, "The international reference ionosphere 2012–a model of international collaboration," *Journal of Space Weather and Space Climate*, vol. 4, p. A07, 2014.

[17] W. Raitt and D. Thompson, "Thermal plasma measurements in space using direct measurements of derivatives of probe current-voltage characteristics," *GEOPHYSICAL MONOGRAPH-AMERICAN GEOPHYSICAL UNION*, vol. 102, pp. 43–48, 1998.

Pedro Alberto Resendiz Lira is currently pursuing the Ph.D. degree with the Department of Physics, University of Alberta, Edmonton, AB, Canada. His current research interests include satellite interaction with space environment.

Richard Marchand is a Professor of Physics with the University of Alberta, Edmonton, AB, Canada, where he does research in computational physics, space physics, and spacecraftenvironment interaction.

Johnathan Burchill is an adjunct assistant professor in the department of physics and astronomy at the University of Calgary. Burchills scientific interests include the physics of upper atmospheric loss to space, ionosphere-thermosphere coupling, and ionospheric physics. He is principal investigator for the European Space Agencys Swarm thermal ion imager in-orbit maintenance and support contract. Burchill develops miniaturized plasma imager instrumentation for sounding rocket and satellite investigations of the ionosphere.

Matthias Förster is working as senior scientist at the GFZ German Research Centre for Geosciences in Potsdam, Germany, as well as at the Max Planck Institute for Solar System Research in Göttingen, Germany.